PERGAMON

Journal of Structural Geology 24 (2002) 1627–1632

JOURNAL OF STRUCTURAL GEOLOGY

www.elsevier.com/locate/jstrugeo

Chemical changes and the development of quartz preferred orientation in zones of crenulation cleavage, Anglesey

John Starkey*

Department of Earth Sciences, University of Western Ontario, London, ON, Canada N6A 5B7

Received 7 June 2001; revised 5 November 2001; accepted 12 November 2001

Abstract

Crenulation cleavage is well developed in rocks of the New Harbour Group of Anglesey, North Wales. Modal and chemical analyses, and a study of the crystallographic orientation of quartz grains, indicate significant differences between the microlithons and the zones of cleavage. The reduction in quartz content and the increase in muscovite observed in the zones of cleavage is accompanied by enrichment in TiO_2, Al_2O_3, Fe_2O_3, MnO, MgO, K_2O and P_2O_5. Conversely SiO_2, CaO and Na_2O are depleted. Mass balance calculations suggest at least a 26% volume decrease in the cleavage zones.

Quartz-rich layers in the microlithons become attenuated when traced into the cleavage zones and the quartz grains are reduced in size and assume a platy habit. The orientation of the quartz *c*-axes is weakly preferred within the microlithons but strongly preferred within the cleavage zones with the development of a single point maximum oriented normal to the plane of cleavage in which the quartz plates lie. This is interpreted as the result of the dissolution of quartz during the formation of the crenulation cleavage with the development of lenticular shapes due to the crystallographic control of the solution rates. Mechanical orientation of the lenses parallel to the cleavage is the likely origin of the preferred crystallographic orientation.

Keywords: Crenulation cleavage; Quartz orientation; Mass balance calculations; Volume loss

1. Introduction

Crenulation cleavage is well developed in the semi-pelites of the New Harbour Group of the Moinian Sequence along the west coast of Anglesey, North Wales, from Porth-y-post to Trearddur Bay (national grid reference SH251790). Two phases of deformation have been recognized in this sequence. The first and major deformation, D_1, strongly affected all rock types. Large F_1 folds are developed in the semi-pelites and greywacke beds and a penetrative axial plane foliation, S_1, is developed. The second deformation, D_2, produced minor folding, F_2, of the S_1 cleavage and a crenulation cleavage, S_2. The metamorphic grade throughout deformation was lower greenschist facies (Shackleton, 1969).

On the hand specimen scale, S_1 is defined by white, quartz-rich layers, approximately 1 mm thick, with intervening thinner layers being rich in phyllosilicates. These layers are folded into microfolds, F_2, with wavelengths of approximately 1–3 cm. In the limbs of the folds the quartz-rich layers are attenuated and often disappear and S_2 cleavage zones are developed, typically 0.5–1.5 cm thick, in which dark green phyllosilicates are concentrated. The rocks display distinct microlithons separated by the spaced crenulation cleavage of the type classified as zonal crenulation cleavage by Gray (1977a).

2. Petrography

The specimen selected for detailed study (number 80/033) contains microlithons approximately 1.5 cm thick separated by cleavage zones approximately 0.5 cm thick (Fig. 1). At one end of the specimen there is a zone of approximately 5 cm, in which the schistosity shows gentler folding with no apparent development of a crenulation cleavage. This will be referred to as the undifferentiated zone in the following discussion. Modal analyses, obtained by averaging data from two thin sections, are presented in Table 1.

The microlithons are composed mainly of quartz and chlorite with lesser amounts of muscovite, plagioclase feldspar (An_8–An_{28}), calcite, sphene, epidote, tourmaline and opaque minerals. The quartz occurs as equidimensional

* Tel.: +1-519-661-3185; fax: +1-519-661-3198.
E-mail address: jstarkey@julian.uwo.ca (J. Starkey).

0191-8141/02/$ - see front matter
PII: S0191-8141(01)00159-6

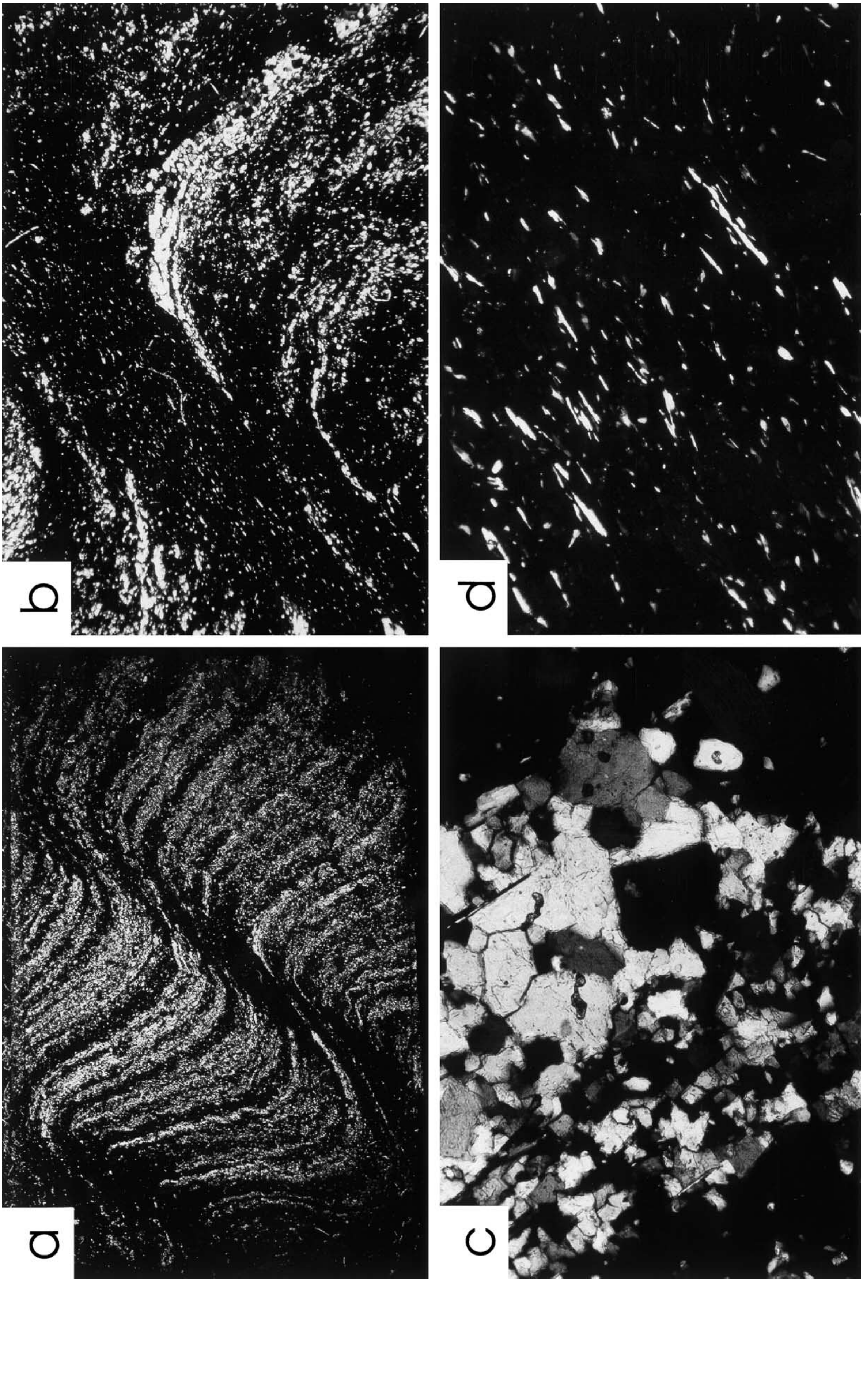

Fig. 1. Photomicrographs between crossed polarizers of a thin section treated with hydrofluosilicic acid to remove all major phases except quartz. (a) The complete thin section showing two microlithons and two cleavage zones. The long dimension is approximately 35 mm. (b) The boundary between a microlithon and cleavage zone. The long dimension is approximately 10 mm. (c) A quartz-rich layer in a microlithon. The long dimension is approximately 1 mm. (d) Quartz within a cleavage zone. The long dimension is approximately 1 mm.

Table 1
Modal analyses of microlithons and cleavage zones

Mineral	Microlithon	Cleavage zone	Enrichment factor
Quartz	60.82	32.64	0.54
Plagioclase	2.03	1.70	0.84
Muscovite	4.39	31.95	7.13
Chlorite	27.88	30.74	1.10
Calcite	1.75	0.85	0.48
Sphene	0.76	1.00	1.32
Accessory minerals (epidote, tourmaline and opaque minerals)	2.38	1.11	0.47

grains up to 0.15 mm in diameter (Fig. 1c). The muscovite is highly chloritized.

The cleavage zones consist dominantly of quartz, muscovite and chlorite with lesser amounts of plagioclase feldspar (An_{24}–An_{32}), calcite, sphene and accessory minerals. Muscovite flakes in the cleavage zone are larger in size than in the microlithons and show no chloritization. However, there is considerable growth of chlorite along the contacts between the microlithons and the cleavage zones. The quartz occurs as relict bands, similar to those in the microlithons (Fig. 1a and b), and as small, isolated lenticular grains less than 0.05 mm in length (Fig. 1d).

3. Chemistry

Chemical analyses of the major elements have been obtained using X-ray fluorescence spectrometry. The material of the microlithons was taken from the hinges of microfolds, as far away as possible from the cleavage zones. The composition of the undifferentiated zone and the mean compositions of the analyzed microlithons and cleavage zones and their specific gravities are shown in Table 2. The enrichment factors listed in Table 2 indicate the enrichment or depletion of elements in the cleavage zones relative to the microlithons. The chemical variations are illustrated in Fig. 2. The chemical composition of the microlithons is similar to that of the undifferentiated zone. However, the composition of the cleavage zones is significantly different. The cleavage zones contain more TiO_2, Al_2O_3, Fe_2O_3, MnO, MgO, K_2O and P_2O_5, and less SiO_2, CaO and Na_2O. Similar compositional variations have been observed in zonal crenulation cleavage by Marlow and Etheridge (1977) and in discrete crenulation cleavages by Gray (1977b).

The composition of the undifferentiated zone is very similar to that of the microlithons and gives, therefore, no evidence for chemical enrichment in the microlithons, as reported by Marlow and Etheridge (1977). The composition of the undifferentiated zone is assumed to represent the approximate composition of the parent rock and is used as the basis for mass balance calculations. Modification of rock chemistry by intercrystalline diffusion during deformation is characterized by non-isochemical and non-isovolumetric reactions (Kerrich et al., 1977). Thus, simple arithmetic differences of the chemical concentrations between the cleavage zones and the microlithons will not represent the true behaviors of rock components during differentiation. Gresens (1967) suggested a two-way mass balance calculation using the chemical analyses of rocks and their specific gravities. Fixing either a volume change factor or the mobility of one component in the reaction provides a unique solution. The data from Table 2 allow a composition–volume diagram to be drawn and volume factors, f_V, to be calculated for the intersections of the composition–volume equations with the zero gain–loss line. The calculated f_V values are as follows:

$$f_v = 0.015X_{SiO_2} + 1.102 \quad (1)$$

$$f_v = 0.932X_{TiO_2} + 0.643 \quad (2)$$

$$f_v = 0.055X_{Al_2O_3} + 0.709 \quad (3)$$

$$f_v = 0.146X_{Fe_2O_3} + 0.740 \quad (4)$$

$$f_v = 9.785X_{MnO} + 0.783 \quad (5)$$

Table 2
Major element analyses for the undifferentiated zone, the microlithons and the cleavage zones. The data for the microlithons and cleavage zones each represent the mean of two analyses, the standard deviation is in parentheses

Major oxide (wt.%)	Undifferentiated zone	Microlithons	Cleavage zones	Enrichment factor
SiO_2	73.85	74.05 (1.83)	65.77 (2.49)	0.89
TiO_2	0.71	0.69 (0.06)	1.05 (0.06)	1.42
Al_2O_3	12.56	12.85 (0.87)	17.73 (1.45)	1.38
Fe_2O_3 [a]	5.08	5.08 (0.46)	6.72 (0.56)	1.32
MnO	0.12	0.08 (0.005)	0.10 (0.015)	1.25
MgO	1.35	1.44 (0.17)	1.97 (0.15)	1.37
CaO	1.19	0.61 (0.30)	0.32 (0.11)	0.52
K_2O	1.12	1.25 (0.31)	3.05 (0.69)	2.44
Na_2O	3.92	3.87 (0.26)	3.15 (0.41)	0.81
P_2O_5	0.09	0.08 (0.01)	0.14 (0.03)	1.75
S.G.	2.728	2.732 (0.019)	2.788 (0.034)	

[a] Fe_2O_3 as total iron.

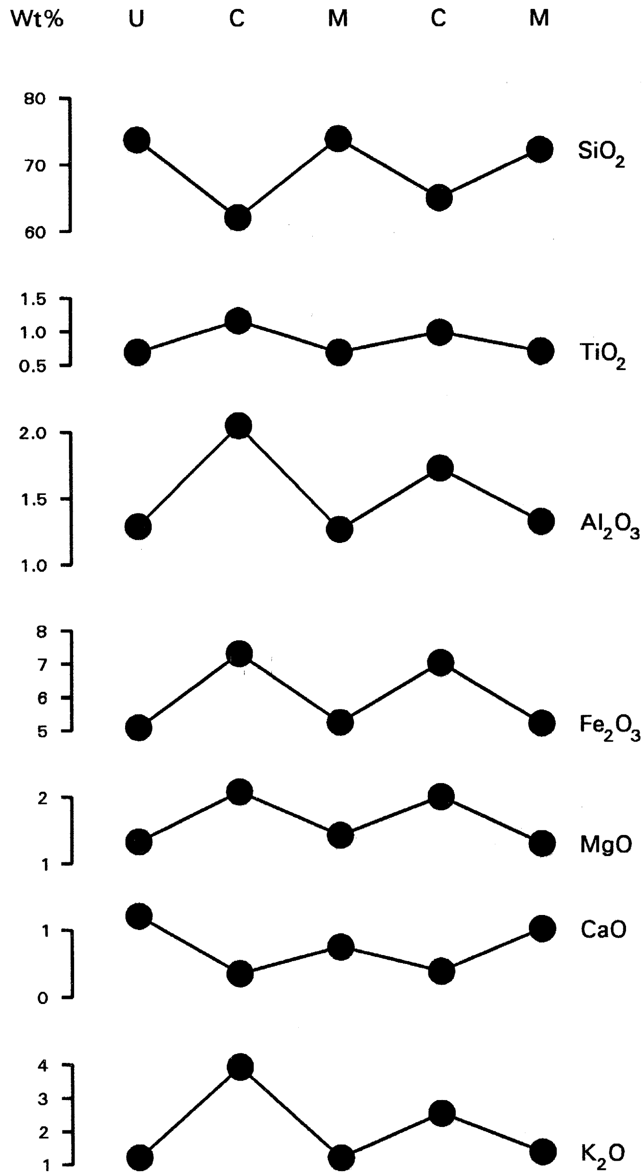

Fig. 2. Variations in major elements in the undifferentiated zone, U, two cleavage zones, C, and two microlithons, M.

$$f_v = 0.497X_{MgO} + 0.715 \quad (6)$$

$$f_v = 3.058X_{CaO} + 1.865 \quad (7)$$

$$f_v = 0.321X_{K_2O} + 0.401 \quad (8)$$

$$f_v = 0.311X_{Na_2O} + 1.202 \quad (9)$$

$$f_v = 6.989X_{P_2O_5} + 0.559 \quad (10)$$

The intersections of the composition-value equations with the isochemical line are illustrated in Fig. 3. The intersections for Al_2O_3, Fe_2O_3 MnO and MgO are closely grouped between $f_v = 0.7$ and 0.8, suggesting that these components were probably relatively immobile during the metasomatism. The mean value $f_v = 0.74$ suggests a volume reduction of at least 26% during the differentiation of the cleavage zone. The data suggest a significant depletion of SiO_2 and addition of K_2O during formation of the crenulation cleavage. A substantial loss of SiO_2 is consistent with the removal of quartz from the cleavage zones and the significant enrichment of K_2O correlates with the concentration of muscovite. As noted above, there is no evidence for chemical enrichment within the microlithons, suggesting that the dissolved material is transported out of the rock as postulated by Bell and Cuff (1989).

4. Quartz crystallographic preferred orientation

The orientations of the *c*-axes of quartz were determined in a microlithon and a cleavage zone using the optical universal stage. A thin section was prepared on plexiglas so that it could be immersed in hydrofluosilicic acid, H_6SiF_6, to remove the layer silicates and feldspar (Kerrich and Starkey, 1979). The resulting thin section is shown in Fig. 1. Fig. 1a illustrates the complete thin section. The quartz-rich layers parallel to S_1 can be traced into, and sometimes across, the cleavage zones. Fig. 1b illustrates the transition of one of the quartz-rich layers at the boundary of the cleavage zone. The layer becomes thinner until it eventually disappears. Fig. 1c and d shows the quartz in a microlithon and a cleavage zone, respectively. Within the microlithon the quartz grains are equidimensional, with a mean grain size up to 0.15 mm. Within the cleavage zone, the quartz located outside preserved remnants of the quartz-rich layers, occurs as small, elongated grains with a maximum length less than 0.05 mm and a typical aspect ratio of approximately 10:1. They show a preferred shape orientation with the long dimensions parallel to the cleavage (Fig. 1d).

Orientation patterns of *c*-axes were prepared following the procedure described by Starkey (1977) using the computer program *Fabric* (Starkey, 1996). The orientation

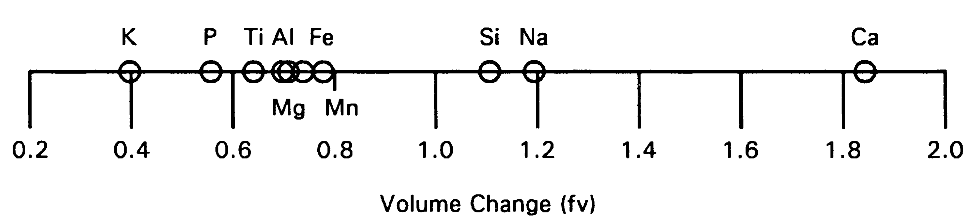

Fig. 3. Intersections of the volume factors, f_V, and the zero gain–loss line on a composition–volume diagram.

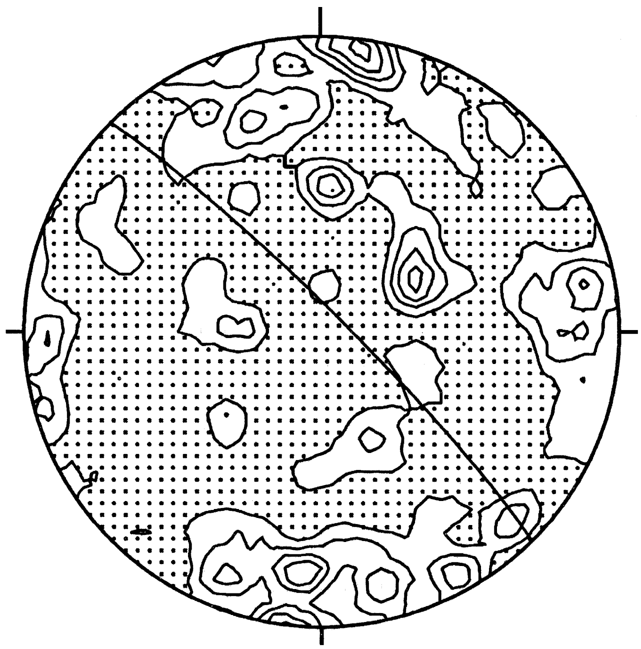

Fig. 4. Orientation pattern of quartz *c*-axes in the microlithon illustrated in Fig. 1c. The great circle represents the cleavage.Sample size 200, contours at 1, 2, 3, 4 and 5 × uniform, empty space is stippled. Upper hemisphere Lambert Equal Area Projection.

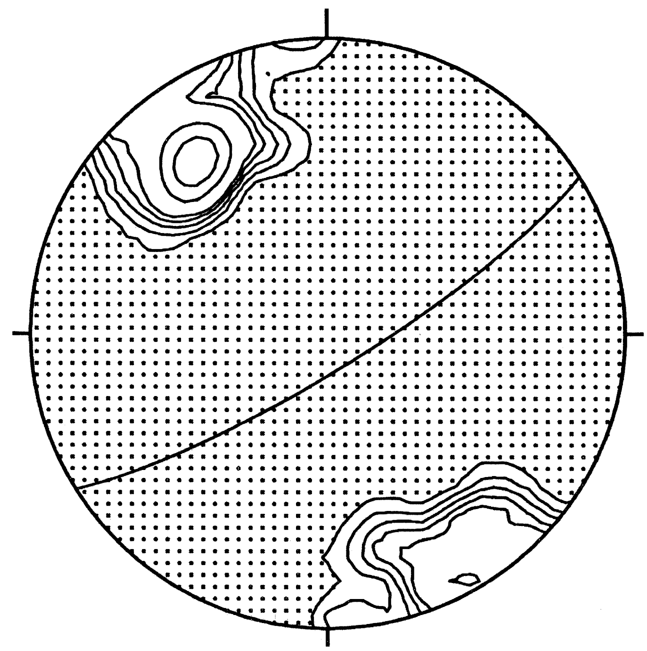

Fig. 5. Orientation pattern of quartz *c*-axes in the cleavage zone illustrated in Fig. 1d. The great circle represents the cleavage. Sample size 100, contours at 1, 2, 3, 4, 5, 10, 15 and 20 × uniform, empty space is stippled. Upper hemisphere Lambert Equal Area Projection.

pattern of the quartz *c*-axes in the microlithon illustrated in Fig. 1c is shown in Fig. 4. There is a weak preferred orientation, with 44% empty space and a maximum concentration of 8 times uniform. Conversely, the quartz *c*-axes in the cleavage zone illustrated in Fig. 1d, display a strong preferred orientation pattern (Fig. 5), with 78% empty space and a maximum concentration of 22 times uniform. The pattern has a single concentration normal to the cleavage.

The preferred orientation pattern observed in the cleavage zone was probably produced by a combination of dissolution and mechanical reorientation. The dissolution of quartz into thin, platy grains is consistent with the known solution rates for quartz (Frondel, 1962) in which the solution rate in the direction of the *c*-axis is several times greater than that in other crystallographic directions and the solution rate parallel to $[10\bar{1}0]$ is least. The result is the development of plates perpendicular to the *c*-axis. Subsequently, the flattening of the rock within the cleavage zone would cause the plates to rotate into the plane of the cleavage defined by the enclosing muscovite flakes, in a manner suggested by the March model (March, 1932). The observed crystallographic preferred orientation is thus a consequence of the preferred shape orientation.

5. Conclusions

Differentiation associated with the formation of crenulation cleavage has removed the most soluble material, predominantly quartz, from the limbs of asymmetric micro-folds. At the same time, muscovite has been added to the cleavage zones. Composition–volume equations suggest that the differentiation was accompanied by a volume reduction of at least 26% in the cleavage zones. The muscovite grew as parallel plates, which define the cleavage. There is no evidence for chemical enrichment within the microlithons, as recorded by Marlow and Etheridge (1977) in rocks from South Australia, although the development of chlorite-rich selvages indicates some chemical redistribution within the cleavage zones.

The dissolution of the quartz was crystallographically controlled to produce small lenticular grains, which were aligned parallel to the cleavage. The orientation of the quartz plates, which are perpendicular to the crystallographic *c*-axis, produced a strong preferred orientation of the *c*-axes perpendicular to the cleavage within the cleavage zones.

Acknowledgements

The chemical analyses were provided by Tsai-way Wu. The support of an operating grant, OGP0003555, from the Natural Sciences and Engineering Research Council of Canada is gratefully acknowledged.

References

Bell, T.H., Cuff, C., 1989. Dissolution, solution transfer, diffusion versus fluid flow and volume loss during deformation/metamorphism. Journal of Metamorphic Geology 7, 425–448.

Frondel, C., 1962. Dana's System of Mineralogy, Vol. III. Silica Minerals. John Wiley and Sons, New York.

Gray, D.R., 1977a. Morphological classification of crenulation cleavage. Journal of Geology 85, 229–235.

Gray, D.R., 1977b. Differentiation associated with discrete crenulation cleavages. Lithos 10, 89–101.

Gresens, R.L., 1967. Composition–volume relationships of metasomatism. Chemical Geology 2, 47–65.

Kerrich, R., Starkey, J., 1979. Chemical removal of feldspars and layer silicates from quartz-bearing rocks for X-ray petrofabric studies. American Mineralogist 64, 452.

Kerrich, R., Fyfe, W.S., Gorman, B.G., Allison, I., 1977. Local modification of rock chemistry by deformation. Contributions to Mineralogy Petrology 65, 183–190.

March, A., 1932. Mathematische Teorie der Regelung nach der Korngestalt bei affiner Deformation. Zeitschrift für Kristallographie 81, 285–297.

Marlow, P.C., Etheridge, M.A., 1977. Development of a layered crenulation cleavage in mica schists of the Kanmantoo Group near Macclesfield, South Australia. Geological Society of America Bulletin 88, 873–882.

Shackleton, R.M., 1969. The Precambrian of North Wales. In: Wood, A. (Ed.). The Precambrian and Lower Paleozoic Rocks of Wales. University of Wales Press, Cardiff, pp. 1–22.

Starkey, J., 1977. The contouring of orientation data represented in spherical projection. Canadian Journal of Earth Sciences 14, 268–277.

Starkey, J., 1996. Presentation of orientation data in spherical projection. In: de Paor, D.G. (Ed.). Structural Geology and Personal Computers. Pergamon, Oxford, pp. 203–215.